


# Circ\_0000079 Decoys the RNA-Binding Protein FXR1 to Interrupt Formation of the FXR1/PRCKI Complex and Decline Their Mediated Cell Invasion and Drug Resistance in NSCLC

Cell Transplantation  
Volume 29: 1–12  
© The Author(s) 2020  
Article reuse guidelines:  
sagepub.com/journals-permissions  
DOI: 10.1177/0963689720961070  
journals.sagepub.com/home/ctj  


Chen Chen<sup>1</sup> , Min Zhang<sup>1</sup>, and Yan Zhang<sup>1</sup>

## Abstract

Nonsmall cell lung cancer (NSCLC) has gradually become one of the deadliest threats to human health and life worldwide. Although reports have shown that circular RNAs (circRNAs) are associated with progression and metastasis of NSCLC, the biological functions of circRNAs during these processes remain largely unknown. Our study showed that circ\_0000079 (CiR79) levels were significantly downregulated in NSCLC patients, especially in cisplatin (DDP)-resistant NSCLC patients, and low circ\_0000079 levels were significantly associated with poor overall survival of NSCLC patients. Then, results from Cell Counting Kit-8 (CCK-8) cell viability assay and transwell cell invasion assay in A549/DDP and H460/DDP cells transfected with pCDH-CiR79 expression vector showed that circ\_0000079 overexpression significantly inhibited cell proliferation and invasion of these DDP-resistant NSCLC cells. The online bioinformatic program StarBase and RNA-binding protein immunoprecipitation predicted and demonstrated that circ\_0000079 could bind with the Fragile X-Related 1 (FXR1) protein rather than with protein kinase C, iota (PRCKI), which was shown to form a complex with FXR1 to promote invasion and growth of NSCLC cells. Co-immunoprecipitation combined with Western blot assays indicated that FXR1 levels were remarkably decreased, but PRCKI levels remained unchanged in pCDH-ciR79 transfected NSCLC cells. Moreover, circ\_0000079 negatively regulated FXR1/PRCKI-mediated phosphorylation of glycogen synthesis kinase 3 $\beta$  and activator protein 1, thus suppressing the protein level of the Snail gene, an important promoter gene regulating cancer cell growth and epithelial-mesenchymal transition. Furthermore, DDP resistance of A549/DDP and H460/DDP cells was inhibited by circ\_0000079 overexpression but was restored by FXR1. Hence, our findings demonstrated that circ\_0000079 might inhibit cell invasion and drug resistance in NSCLC by interrupting the formation of the FXR1/PRCKI complex by interacting with FXR1, and circ\_0000079 could act as a potential biomarker and therapeutic target for NSCLC.

## Keywords

circ\_0000079, NSCLC, cisplatin resistance, FXR1/PRCKI, RNA–protein interaction

## Introduction

Lung cancer is the leading cause of cancer-related mortality worldwide, and more than 80% of lung cancers are classified as nonsmall cell lung cancer (NSCLC)<sup>1,2</sup>. NSCLC consists of squamous cell carcinoma, large cell carcinoma, and adenocarcinoma, and most patients with advanced NSCLC have a local invasion and/or distal metastasis at presentation<sup>3</sup>. Although cisplatin (DDP)-based chemotherapy is an effective method used in the treatment of advanced malignancies, which is one of the first-line chemotherapeutic agents for

<sup>1</sup> Department of Pathology, the Second Affiliated Hospital of Zhengzhou University, Zhengzhou, P. R. China

Submitted: March 18, 2020. Revised: July 24, 2020. Accepted: September 3, 2020.

### Corresponding Author:

Chen Chen, Department of Pathology, the Second Affiliated Hospital of Zhengzhou University, No. 2 of Jingba Road, Zhengzhou 450000, P. R. China.

Email: chen\_chenzz@126.com



Creative Commons Non Commercial CC BY-NC: This article is distributed under the terms of the Creative Commons Attribution-NonCommercial 4.0 License (<https://creativecommons.org/licenses/by-nc/4.0/>) which permits non-commercial use, reproduction and distribution of the work without further permission provided the original work is attributed as specified on the SAGE and Open Access pages (<https://us.sagepub.com/en-us/nam/open-access-at-sage>).

NSCLC, the 5-year survival rate is still only 15%, and the effectiveness of the treatment remains limited due to an inherent tumor resistance of NSCLC<sup>4-6</sup>. Therefore, identifying biomarkers for drug-resistant NSCLC detections and treatment targets to facilitate the development of new drugs are urgently needed.

Circular RNAs (circRNAs) are a class of novel endogenous noncoding RNAs, which are described as RNA molecules in the loop structure generated from the aberrant splicing of the transcripts<sup>7,8</sup>. Unlike linear RNAs, circRNAs are characterized by covalently closed continuous loop structures with neither 5' to 3' polarity nor a polyadenylated tail, and they are highly represented *in vivo* compared with their linear counterparts and are predominantly in the cytoplasm and also can be sorted into exosomes<sup>9</sup>. Currently, large-scale studies revealed that circRNAs are vital to many biological processes in various tumors, such as cell proliferation, invasion, and differentiation of lung cancers<sup>10,11</sup>. For instance, Zong et al. discovered that circ\_102231 inhibition significantly suppressed lung cancer cell proliferation and invasion ability *in vitro*<sup>12</sup>; Zhu et al. found that hsa\_circ\_0013958 promoted cell proliferation and invasion and inhibited cell apoptosis in NSCLC<sup>13</sup>; Zhao et al. showed that circFADS2 was an effective tumor promoter in lung cancer progression, and its functions were performed by regulating the expression of miR-498<sup>8</sup>. Growing evidence has suggested that circRNAs could be a novel candidate for molecular therapeutic research of NSCLC, but the roles of massive circRNAs in tumor carcinogenesis remain largely unknown.

In the present study, we found that circ\_0000079 expression was decreased in NSCLC tissues and was associated with a poor survival rate. Further experiments showed that circ\_0000079 could bind with the fragile X-related 1 (FXR1) protein but could not with its complex-partner protein kinase C, iota (PRKCI), to suppress invasion and drug resistance of NSCLC cells.

## Materials and Methods

### Patients and Clinical Samples

A total of 204 tissue samples, including 26 nontumor tissue samples (control) derived from pulmonary laceration patients who underwent pulmonary laceration repair and 178 NSCLC tissue samples derived for NSCLC patients who underwent radical resection, were collected at the Second Affiliated Hospital of Zhengzhou University (Zhengzhou, China) from May 2011 to March 2014. None of the subjects had received any chemotherapy and radiotherapy prior to surgery. Patients at the age of less than 12 years, or with organ dysfunction (liver, kidney, cardiovascular), previous or complicated with malignant tumors, or with serious systemic disorders, such as severe infection or immunodeficiency, were excluded from this study. All of these patients were treated with cisplatin (DDP)-based

chemotherapy after surgery according to the National Comprehensive Cancer Network guideline every 3 weeks for four cycles. Patients with progressive disease (PD) or with recurrence <6 months after surgery were defined as DDP-resistant, whereas those without PD and with recurrence >12 months after surgery were defined as nonresistant. We followed up the patients by telephone or outpatient service from May 2011 to June 2019. The follow-up contents included survival, cause of death, time of death, location of metastasis, time of metastasis, and treatment plan. There were 82 NSCLC patients who are sensitive to DDP treatment and 96 NSCLC patients with DDP chemoresistance. These resected specimens were rapidly frozen under -80 °C. Tissue sample usage was approved by the Ethics Committees of the Second Affiliated Hospital of Zhengzhou University, and written informed consent was obtained from all the participants.

### Cell Lines and Cell Culture

BEAS-2B, HBE, A549, H460, A549/DDP, and H460/DDP cells were purchased from Cell Bank of the Chinese Academy of Science (Shanghai, China). The cells were maintained in Dulbecco's Modified Eagle Medium (DMEM) or Roswell Park Memorial Institute-1640 medium (Gibco, Grand Island, New York State, USA) supplemented with 10% fetal bovine serum (FBS; Gibco), containing 100 U/ml penicillin and 100 mg/ml streptomycin. Both cell lines were incubated at 37 °C in a humidified atmosphere of 5% carbon dioxide. DDP-resistant NSCLC cells were cultured in a medium supplemented with DDP at a final concentration of 2 μM, to maintain drug resistance. DDP was purchased from Sigma Chemical Co (St. Louis, MO, USA).

### Cell Proliferation Assay

Cell Counting Kit-8 (CCK-8; Dojindo, Japan) was performed to test cell proliferation. Briefly,  $1 \times 10^4$  cells were seeded into six-well plates. For each well, 200 μl CCK-8 solution was added. Then, the cells were incubated at 37 °C for 2 h. The absorbance at 450 nm was measured by using a spectrophotometer every day.

### Transwell Cell Invasion Assay

The invasion of NSCLC cells was detected by the transwell cell invasion assay. In brief,  $5 \times 10^4$  NSCLC cells were suspended in 200 mL of serum-free DMEM. Chambers (8 μm, BD Biosciences, Franklin Lakes, NJ, USA) were plated with BD BioCoat Matrigel according to the manufacturer's protocol. NSCLC cells were incubated for 48 h at 37 °C. After incubation, the upper surface of the membrane was wiped with a cotton tip, and the cells attached to the lower surface were stained with crystal violet for 5 min. The number of cells on the lower surface was counted under a light microscope in five random fields.

### RNA Extraction and Quantitative PCR (qPCR)

Total RNA was isolated from tissues and cells by using the TRIzol (Invitrogen, Carlsbad, CA, USA). Single-stranded cDNA was synthesized with the PrimeScript Reagent Kit (Promega, Madison, USA). The cDNA was carried out starting from 100 ng of total RNA. The relative expression levels of circRNA and miRNA were detected by using the SYBR Green Master Mix (Takara Biotechnology, Dalian, China) in Step One Plus Real-Time PCR system (Applied Biosystem, Foster City, CA, USA). Circ\_0000079 was validated via PCR using divergent and convergent primers. Glyceraldehyde 3-phosphate dehydrogenase was used as an endogenous control. Briefly, 500 ng of total RNA was reversely transcribed into cDNA with random primers in a total volume of 20  $\mu$ l. The reactions were initiated in a 96-well optical plate at 95 °C for 30 s, followed by 40 cycles of 95 °C for 5 s and 60 °C for 20 s.

### Transfection

To recapitulate circRNA, the genomic region for circ\_0000079 with its flanking introns was amplified using PrimerSTAR Max DNA Polymerase Mix (Takara). The PCR products were inserted into the pcDNA3.0 vector. Small interfering RNAs (siRNAs) against circ\_0000079 and FXR1 recombinant protein were constructed and purchased from GenePharma (Shanghai, China). All vectors were verified by sequencing. All cell transfections were performed by using Lipofectamine 3000 (Invitrogen) according to the manufacturer's protocol.

### RNA-Binding Protein Immunoprecipitation Assay (RNA-IP)

In RNA-IP assays, cells were harvested when they reached 70% to 80% confluence. In brief,  $10^7$  cells were washed in ice-cold phosphate-buffered saline (PBS), lysed in Tris-hydrochloric acid (HCl), pH 7.5, buffered with 1% Triton or digitonin containing protease inhibitors, and incubated with 5  $\mu$ g of primary antibody at 4 °C for 2 h. A total of 40  $\mu$ l of 50% slurry of protein A-Sepharose (GE Healthcare, Chicago, USA) was added to each sample, and the mixtures were incubated at 4 °C for 4 h. The pellets were washed with 3  $\times$  PBS and resuspended in 0.5 ml Tri Reagent (Sigma-Aldrich). The coprecipitated RNA eluted in aqueous solution was analyzed by qPCR to prove the presence of binding products using their respective primers.

### Pull-Down Assay with Biotinylated RNA

The cell lines were transfected with biotinylated RNA (50 nM) and harvested 48 h after transfection. The cells were washed with PBS followed by brief vortex and incubated in a lysis buffer (20 mM Tris, pH 7.5, 200 mM sodium chloride [NaCl], 2.5 mM magnesium chloride, 0.05% Igepal, 60 U/ml Superase-In [Ambion, USA], 1 mM DTT, protease

inhibitors) on ice for 10 min. The lysates were precleared by centrifugation, and 50  $\mu$ l of the samples were aliquoted for input. The remaining lysates were incubated with M-280 streptavidin magnetic beads (Sigma). The beads were coated with RNase-free BSA and yeast total RNA (both from Sigma). The beads were incubated at 4 °C for 3 h, washed twice with ice-cold lysis buffer, three times with the low salt buffer (0.1% sodium dodecyl sulfate [SDS], 1% Triton X-100, 2 mM EDTA, 20 mM Tris-HCl pH 8.0, 150 mM NaCl), and once with the high salt buffer (0.1% SDS, 1% Triton X-100, 2 mM EDTA, 20 mM Tris-HCl pH 8.0, 500 mM NaCl). The bound RNAs were purified by Trizol for the analysis.

### Co-Immunoprecipitation (co-IP)

NSCLC cells were transfected 1  $\mu$ g/ml pCDH-ciR79 (GenePharma), 100 nM siCirc\_0000079 (GenePharma), or corresponding negative controls (GenePharma) for 48 h, and next were incubated with anti-PRKCI antibody (1:500, Abcam, ab154681) or immunoglobulin G (IgG; 1:500, Abcam, ab6728) for 24 h, then subjected to co-IP. For IP of transfected or normal NSCLC, the cells were lysed in Tris-HCl, pH 7.5, buffered with 1% Triton or digitonin containing protease inhibitors. Supernatant was incubated with appropriate antibody (2  $\mu$ g) for at least 90 min at 4 °C followed by incubation for an additional 90 min with Protein A-Sepharose beads. Beads were washed with lysis buffer three times, incubated for 5 min at 95 °C with Laemmli buffer, and subjected to Western Blot analysis.

### Western Blot

Western Blot was performed according to the following procedure. Cells were lysed in total protein lysis buffer (Thermo Fisher Scientific, Waltham, MA, USA) supplemented with protease and phosphatase inhibitor for 1 h at 4 °C. The protein concentration was measured using a BCA protein assay reagent kit (Sigma). Proteins were separated by 10% SDS polyacrylamide gel electrophoresis and then transferred to a polyvinylidene difluoride membrane (Millipore, Boston, MA, USA). After blocking in 5% skim milk for 1 h, the anti-PRKCI antibody (1:500, Abcam, ab154681), anti-FXR1 antibody (1:500, Abcam, ab51970), anti-proliferating cell nuclear antigen (PCNA) antibody (1:500, Abcam, ab29), anti-B-cell lymphoma 2 (Bcl-2) antibody (1:500, Abcam, ab32124), anti-E-cadherin antibody (1:500, Abcam, ab1416), anti-Snail (1:400, Cell Signaling Technology), anti-glycogen synthesis kinase 3 $\beta$  (GSK3 $\beta$ ; 1:300, Cell Signaling Technology), anti-p-GSK3 $\beta$  (1:200, Cell Signaling Technology), anti-activator protein -1 (AP-1:350, Cell Signaling Technology), anti-p-AP-1 (1:200, Cell Signaling Technology), anti-multidrug resistance-associated protein-1 (MRP-1; 1:350, Cell Signaling Technology), anti-lung resistance-associated protein (LRP; 1:300, Cell Signaling Technology), and anti-vimentin antibody (1:500, Abcam, ab20346) were used in this work.

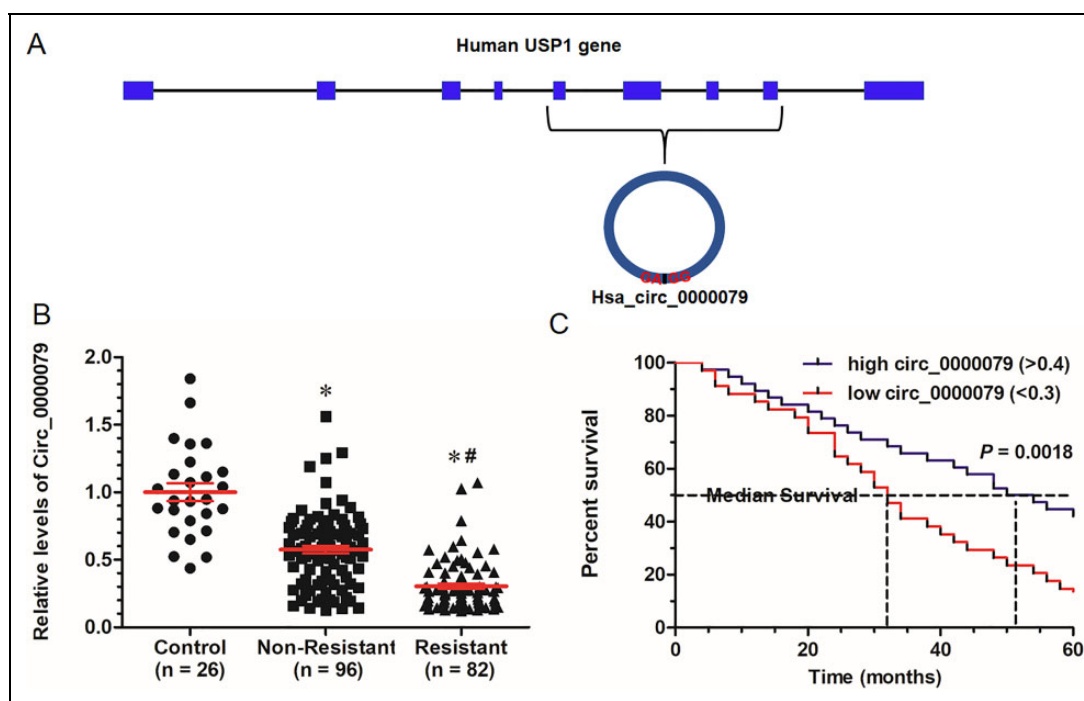


**Fig. 1.** Circ\_0000079 expression profile in NSCLC tissues and its association with patients' prognosis. (A) The schematic diagram for the transcription and splicing process of hsa\_circ\_0000079 (abbreviated as CiR79 in the figures). (B) Qualitative PCR was used to detect the expression of circ\_0000079 in lung tissues of nonresistant NSCLC patients ( $n = 96$ ), DDP-resistant NSCLC patients ( $n = 82$ ), and adjacent normal lung tissues ( $n = 26$ ) (the average expression level of the control group was defined as 1). (C) The Kaplan–Meier survival analysis and log-rank test showed that patients with high circ\_0000079 levels ( $n = 34$ ) elevated survival times compared with patients with low circ\_0000079 levels ( $n = 36$ ). The median survival time for patients with high and low expression of circ\_0000079 was 52 months as compared with 32 months, respectively ( $P = 0.0018$ ). Each level group contains half nonresistant NSCLC and half-resistant NSCLC patients. \* $P < 0.05$  compared with the control group, # $P < 0.05$  compared with nonresistant group. DDP: cisplatin; NSCLC: nonsmall cell lung cancer.

After incubating with the primary antibodies overnight at 4 °C, the membranes were incubated with corresponding secondary antibodies for 1 h at room temperature. Protein bands were visualized using SuperSignal West Femto Maximum Sensitivity Substrate solution (Thermo Fisher Scientific) and captured on X-ray films.

### Statistical Analysis

All experiments were repeated at least three independent times. Statistical analysis was performed using SPSS 22.0 software (SPSS, Chicago, IL, USA) or GraphPad Prism Version 6 (GraphPad Software Inc., San Diego, CA, USA). The data were expressed as the mean  $\pm$  SEM.  $P < 0.05$  was considered statistically significant.

## Results

### Circ\_0000079 Expression Profile in NSCLC Tissues and its Association with Patients' Prognosis

As shown in Fig. 1A, hsa\_circ\_0000079 is a circular RNA with 1226 nt in spliced sequence length. Its gene is located at chr1:62908829-62914337 and generated by circularization of the fifth to ninth exons of ubiquitin-specific protease 1

(USP1) gene. Qualitative PCR was used to detect the relative expression of circ\_0000079 in 96 nonresistant NSCLC lung tissues, 82 cisplatin (DDP)-resistant NSCLC lung tissues, and 26 adjacent normal lung tissues. The results showed that circ\_0000079 levels were the lowest in DDP-resistant NSCLC cells compared with nonresistant NSCLC cells and noncancerous cells, and circ\_0000079 levels were highest in noncancerous cells, which imply that circ\_0000079 was associated with the DDP-resistant NSCLC (Fig. 1B). The clinicopathologic characteristics of the DDP-resistant and nonresistant patients were listed in Table 1, which revealed that there is no difference in age, sex, tumor size, and metastasis between the resistant and nonresistant patients, but resistant patients displayed much lower circ\_0000079 level, deeper invasion, and poorer differentiation degree. To assess the correlation of circ\_0000079 expression with the survival rate of the patients, the expression levels of circ\_0000079 in NSCLC patient lung tissues were categorized as the high-level group ( $n = 34$ ) and low-level group ( $n = 38$ ), and each group accounted for half of nondrug resistance NSCLC patients and half of drug-resistance NSCLC patients. Compared with the circ\_0000079 high expression group, Kaplan–Meier survival curves showed that the patients with low expression of circ\_0000079 had a lower 5-year overall

**Table 1.** Clinicopathological Characteristics of the Non-Resistant and Resistant Patients.

Parameters	Nonresistant cases	Resistant cases	$\chi^2$ -value	P-value
<b>Age distribution</b>	96 (54.1 ± 10.8)	82 (52.9 ± 9.9)	0.008	0.929
≤60	58	49		
>60	38	33		
<b>Sex</b>				
Male	50	45	0.139	0.709
Female	46	37		
<b>CiR79 level</b>				
≤0.5 fold of control	37	71	42.781	<0.001***
>0.5 fold of control	59	11		
<b>Distal metastasis</b>				
Negative	43	32	0.603	0.437
Positive	53	50		
<b>Tumor size</b>				
≤ 5 cm	55	40	1.287	0.257
> 5 cm	41	42		
<b>Depth of invasion</b>				
N0/N1	51	31	4.178	0.041*
N2/N3	45	51		
<b>Differentiation</b>				
Well/Moderately	54	29	7.751	0.005**
Poorly	42	53		

\* $P < 0.05$ . \*\* $P < 0.01$ . \*\*\* $P < 0.001$ .

survival rate and shorter median survival time (52 vs 32 months,  $P = 0.0018$ ) (Fig. 1C). These results indicated that circ\_0000079 may participate in the development and progression of human NSCLC.

### Increased Circ\_0000079 Expression Inhibited Cell Proliferation and Invasion of DDP Resistance NSCLC Cells

To explore whether circ\_0000079 play a role in the development of NSCLC, six different types of cells were selected as research representatives in the following studies, including two human normal lung epithelial cell lines (BEAS-2B, HBE), two nonresistant NSCLC cell lines (A549, H460), and two DDP-resistant NSCLC cell strains (A549/DDP, H460/DDP). qPCR analysis showed that circ\_0000079 levels were dramatically decreased in NSCLC cell lines, especially in cells with DDP resistance, compared with two human normal lung epithelial cell lines (Fig. 2A) ( $n = 6$ ). As shown in Fig. 2B, the level of circ\_0000079 in the pCDH-ciR79 transfected cells was significantly increased in a dose-dependent manner compared with the vehicle control.

As shown in Fig. 2C, D, CCK-8 cell count assay and transwell cell invasion assay showed a significant decrease in growth and invasion of A549/DDP and H460/DDP cells when circ\_0000079 was overexpressed, compared with the control group ( $n = 6$ ). Therefore, our data suggested that circ\_0000079 plays an important role in the progression of NSCLC, and circ\_0000079 suppressed cell proliferation and invasion of DDP-resistant NSCLC *in vitro*.

### Circ\_0000079 Could Bind with FXR1 But Not with PRKCI in NSCLC

To investigate the mechanism of circ\_0000079 involved in NSCLC tumorigenesis, the online bioinformatic program StarBase was used to search circ\_0000079 target proteins, and we found that circ\_0000079 may interact with the FXR1 protein. FXR1 is an RNA-binding protein, which coordinates elaborate networks of RNA-protein and protein-protein interactions that link RNA metabolism to signal transduction pathways. Then, we speculated that circ\_0000079 might suppress cell invasion and drug resistance in NSCLC by interacting with FXR1. However, large-scale studies had revealed that FXR1 was highly expressed in many human cancers and its overexpression is associated with poor prognosis in NSCLC, and further investigations showed that FXR1 could drive NSCLC progression *in vitro* and *in vivo* through binding with PRKCI<sup>14-16</sup>. Thus, we investigated the relation between circ\_0000079 and FXR1/PRKCI in drug-resistant NSCLC cells by using RNA-IP and RNA pull-down. RNA-IP combined with qPCR analyses showed that an abundant amount of circ\_0000079 was observed in the protein-RNA complex precipitated by FXR1-antibody, but not in that precipitated by PRKCI antibody (Fig. 3A). The circ\_0000079-probe-based RNA pull-down combined with Western blotting assays showed that circ\_0000079 could bind with FXR1 but not PRKCI (Fig. 3B). Our data suggested that circ\_0000079 can interact with FXR1 rather than with PRKCI in NSCLC cells. Hence, we speculated that circ\_0000079 might block the formation of the FXR1/PRKCI complex via interaction with FXR1.

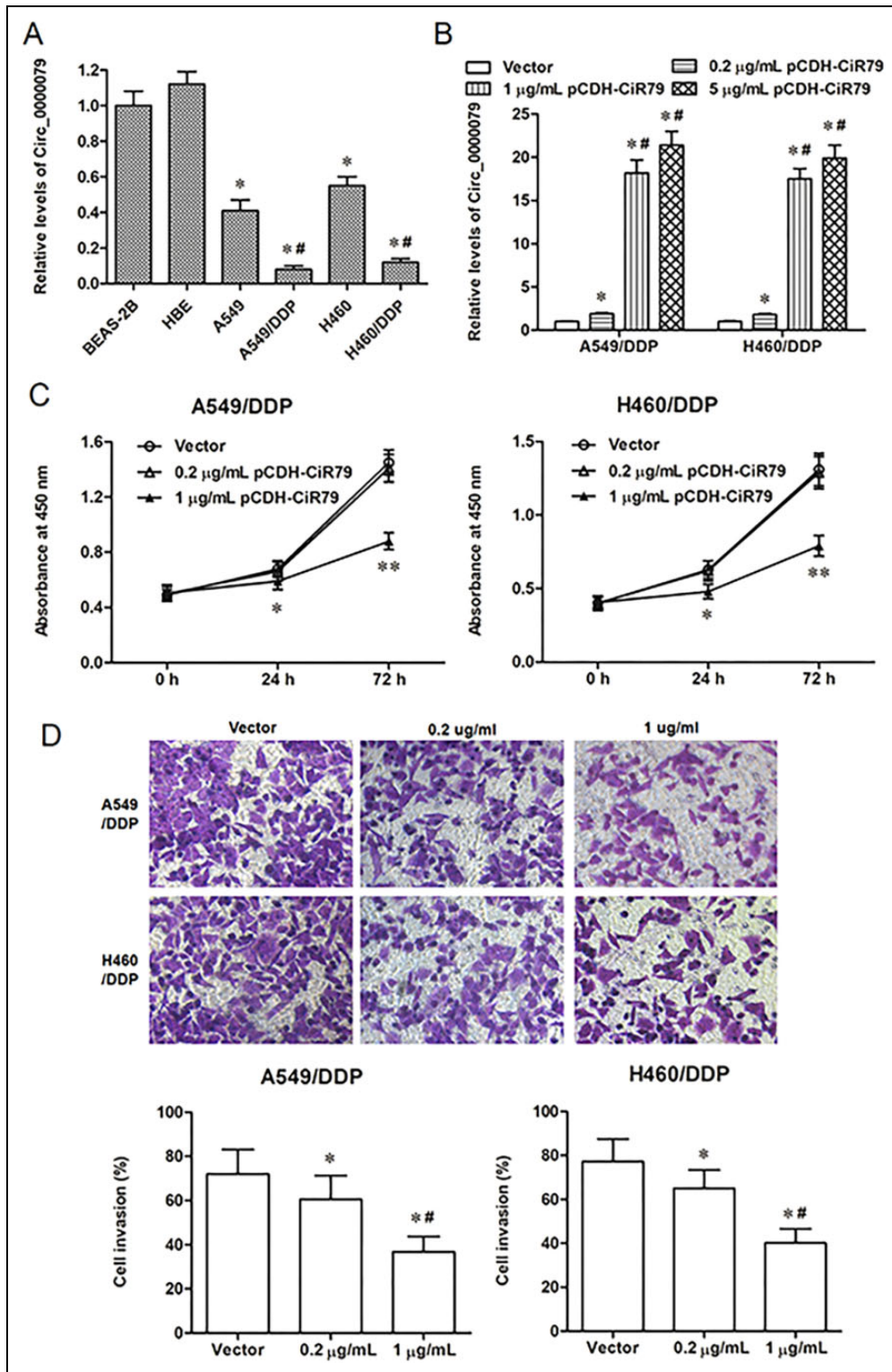


**Fig. 2.** Increased circ\_0000079 expression inhibited cell proliferation and invasion of DDP resistance NSCLC cells. (A) Comparison of circ\_0000079 levels among human normal lung epithelial cell lines (BEAS-2B and HBE), NSCLC cell lines (A549 and H460), and DDP-resistant NSCLC cell lines (A549/DDP and H460/DDP) ( $n = 6$ ).  $*P < 0.05$  compared with human normal lung epithelial cell lines and  $^{\#}P < 0.05$  compared with NSCLC cell lines. (B) A549/DDP and H460/DDP were transfected with 0.2, 1, and 5  $\mu$ g/ml pCDH-ciR79 for 72 h, respectively. The expression of Circ\_0000079 after transfection was detected by qualitative PCR ( $n = 6$ ).  $*P < 0.05$  compared with vector.  $^{\#}P < 0.05$  compared with 0.2  $\mu$ g/ml pCDH-ciR79. (C-D) A549/DDP and H460/DDP cell lines were transfected with 0.2 and 1  $\mu$ g/ml pCDH-ciR79 for 72 h, respectively. (C) The proliferation status of A549/DDP and H460/DDP cell lines after transfection was detected by CCK-8. (D) Transwell cell invasion assay for the determination of invasion of A549/DDP and H460/DDP cells after transfection.  $*P < 0.05$  compared with the control group.  $^{\#}P < 0.05$  compared with 0.2  $\mu$ g/ml pCDH-ciR79. CCK-8: cell counting kit-8; DDP: cisplatin; NSCLC: nonsmall cell lung cancer.



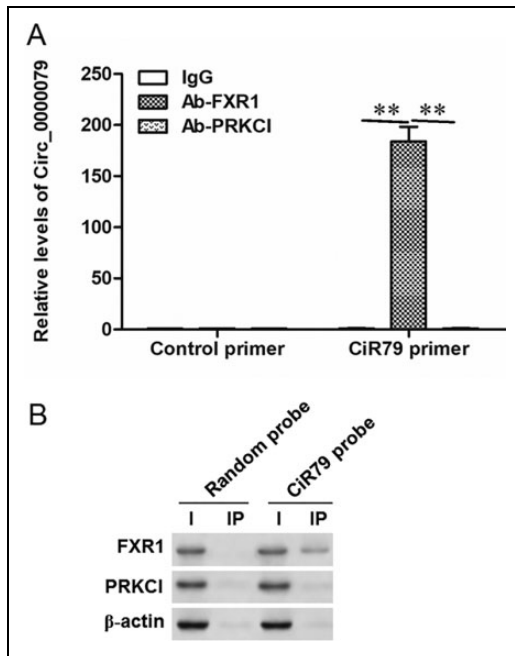


**Fig. 3.** Circ\_0000079 could bond with FXR1 but not with PRKCI in NSCLC. The online bioinformatic program StarBase predicted circ\_0000079 could combine the protein of FXR1. The lysates from resistant NSCLC cells were subjected to RNA-binding protein IP with antibodies against FXR1 and PRKCI, and then qualitative PCR was used to detect the interaction between circ\_0000079 and FXR1, PRKCI by the control primer and circ\_0000079 primer. Ab as the antibody and IgG as the negative control in the experiment.  $**P < 0.01$ . (B) The lysates prepared from resistant NSCLC cells were transfected with biotinylated circ\_0000079 probe or a random oligo probe (50 nM), harvested 48 h after transfection, and then subjected to RNA pull-down and Western Blot analysis. I, 30% samples were loaded) and P, 100% samples were loaded ( $n = 6$ ). FXR1: fragile X-related 1 protein; I: input; IgG: immunoglobulin G; IP: immunoprecipitation; NSCLC: nonsmall cell lung cancer; P: pellet; PRKCI: protein kinase C: iota.

### Circ\_0000079 Decoyed FXR1 to Interrupt Formation of the FXR1/PRKCI Complex and Negatively Regulated Snail Expression

To verify our hypothesis above, we performed co-IP experiments and found that the expression levels of FXR1 were remarkably decreased in pCDH-ciR79 transfected NSCLC cells but remarkably increased in the siCirc\_0000079-transfected NSCLC cells compared with the control. However, PRKCI levels remained unchanged in response to changed circ\_0000079 levels ( $n = 6$ ) (Fig. 4A). Our results further indicated that upregulated circ\_0000079 could suppress the binding of FXR1 and PRKCI in NSCLC. To explore whether circ\_0000079 inhibited NSCLC progression through interrupting FXR1/PRKCI, we next investigated the effect of changed circ\_0000079 and FXR1 levels on the expression of the key proteins regulating cell invasion and resistance of NSCLC, including Bcl2, vimentin, and

E-cadherin. Western Blot analysis displayed that Bcl-2 and vimentin levels were both declined in pCDH-ciR79-transfected cells and strikingly raised in pCirc\_0000079-transfected cells, while they showed the normal level in cells co-transfected with circ\_0000079 and FXR1, compared with the control. On the contrary, E-cadherin levels were dramatically raised in cells transfected with pCDH-ciR79 but reduced in cells transfected with siCirc\_0000079, while it was rescued in cells co-transfected with circ\_0000079 and FXR1, compared with the control (Fig. 4B). The FXR1/PRKCI complex has been shown to positively regulate Snail through activating the GSK3 $\beta$  and AP-1. We then investigated the effect of circ\_0000079 on phosphorylation levels of GSK3 $\beta$  and AP-1. Western blotting showed that circ\_0000079 negatively regulated phosphorylation of GSK3 $\beta$  and AP-1, thus suppressing the expression Snail, a famous regulator in the promotion of cancer cell growth and epithelial-mesenchymal transition (EMT) (Fig. 4C). Together, our data suggested that circ\_0000079 might suppress the carcinogenesis of NSCLC by interrupting the formation of the FXR1/PRKCI complex by bonding with FXR1.

### FXR1 Could Restore the DDP Resistance Reduced by Circ\_0000079

The study further examined whether circ\_0000079 suppressed drug resistance of NSCLC cells by interaction with FXR1. First, A549, A549/DDP, and pretreated A549/DDP cells were treated with DDP at the indicated concentration for 48 h before subjected to CCK-8 analysis. The results showed that the cell invasion of all cells decreased with the increase of DDP added concentration (Fig. 5A). Then, it can be seen more intuitively in bar graphs: IC<sub>50</sub> for DDP of A549/DDP was significantly higher than A549/DDP transfected with 0.2  $\mu$ g/ml pCDH-ciR79 but had no difference with A549/DDP transfected with 0.2  $\mu$ g/ml pCDH-ciR79 and 5  $\mu$ g/ml FXR1 (Fig. 5B). As expected, four types of H460 cells had the same consequences under the same treating condition (Fig. 5C, D). Consistently, the levels of MRPs, including MRP-1 and LRP, were also suppressed by ciR79 overexpression and rescued by FXR1 (Fig. 5E). Overall, our studies suggested that circ\_0000079 overexpression could inhibit the resistance of NSCLC cells by decoying FXR1.

## Discussion

CircRNAs are a recently discovered type of noncoding RNAs, which existed extensively in mammalian cells and have been regarded as productions by circularization of exons resulting from errors during post-transcriptional processing<sup>17,18</sup>. Emerging evidence revealed that circRNAs exhibited tissue-specific and developmental-specific expression pattern and played crucial roles in multiple cellular processes of many cancers<sup>11,18,19</sup>. Circ\_0000079 was first detected in human HEK293 cells and was first reported in

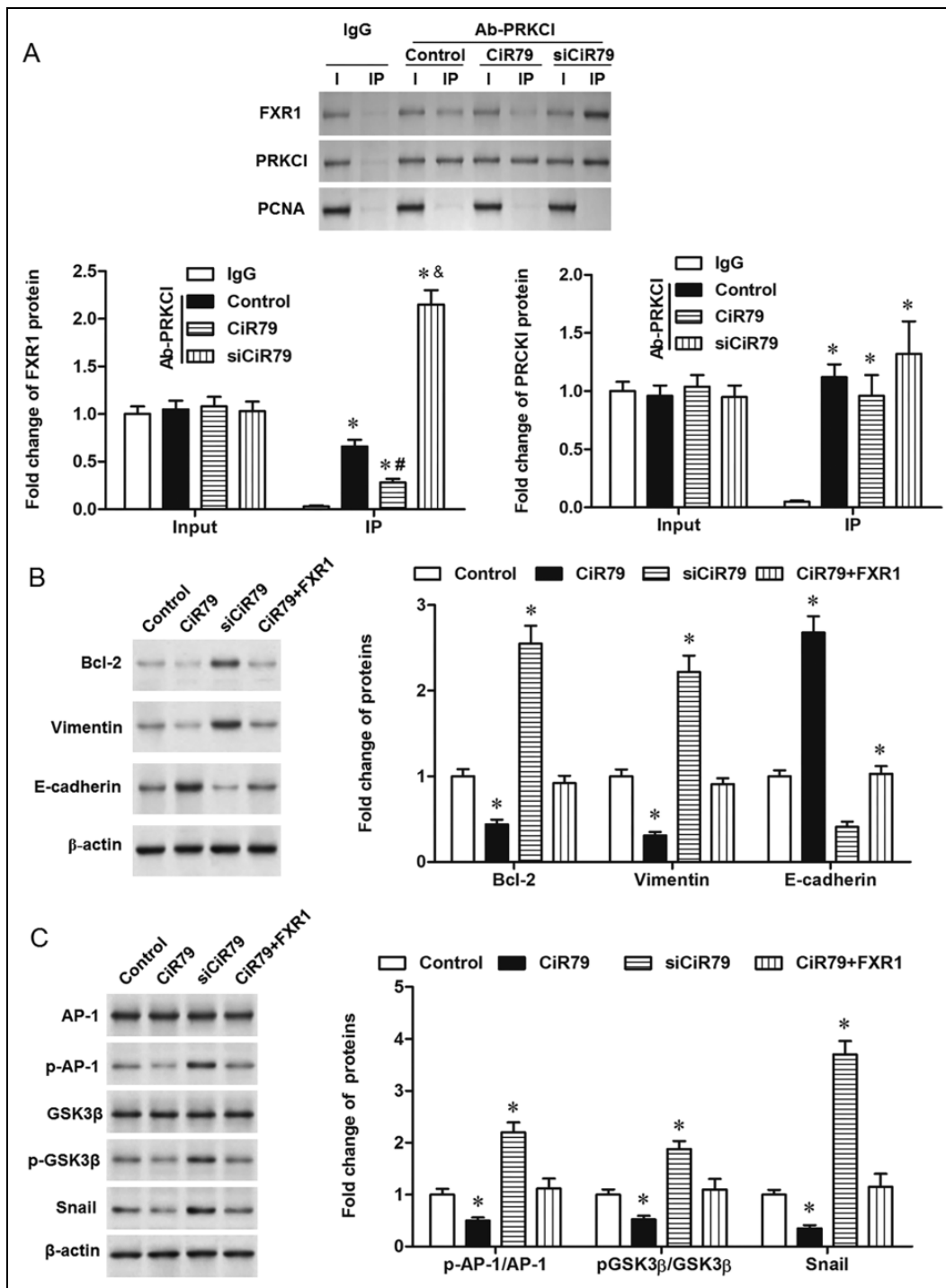


**Fig. 4.** Circ\_0000079 decoyed FXR1 to interrupt the formation of the FXR1/PRKCI complex. (A) The NSCLC cells prepared for co-IP were transfected 1  $\mu$ g/ml pCDH-ciR79, siCirc\_0000079, or vector for 48 h, and then incubated with PRKCI antibody or IgG for 24 h. Lysates from preprocessed NSCLC cells were subjected to Western Blot analysis with antibodies against FXR1, PRKCI, and PCNA to study on the binding of circ\_0000079 and FXR1 and PRKCI. The protein-level quantification analyses of FXR1 and PRKCI are displayed in the right panel ( $n = 6$ ). As shown, PCNA was the control, and IgG was the negative control. I, 30% samples were loaded; IP, 100% samples were loaded. \* $P < 0.05$  compared with IgG group. # $P < 0.05$  and & $P < 0.05$  compared with the control group. The NSCLC cells subjected to Western Blot after transfected 1  $\mu$ g/ml pCDH-ciR79 or 100 nM siCirc\_0000079 or 5  $\mu$ g/mL FXR1 recombination protein for 48 h. (B) Expression of the apoptosis and invasion-related marker genes in NSCLC cells, including Bcl2, vimentin, and human epithelial cadherin (E-cadherin) was detected with Western blotting, and their protein-level quantification analyses are displayed in the right panel ( $n = 6$ ). (C) The phosphorylation levels of GSK3 $\beta$  and AP-1 and expression of Snail were detected with Western blotting.  $\beta$ -actin was used as an invariant internal control for calculating protein-fold changes. \* $P < 0.05$  compared with the control group. AP-1: activator protein 1; Bcl2: B-cell lymphoma 2; FXR1: fragile X-related 1 protein; GSK3 $\beta$ : glycogen synthesis kinase 3 $\beta$ ; I: input; IP: immunoprecipitation; NSCLC: nonsmall cell lung cancer; PCNA: proliferating cell nuclear antigen; PRKCI: protein kinase C: iota.



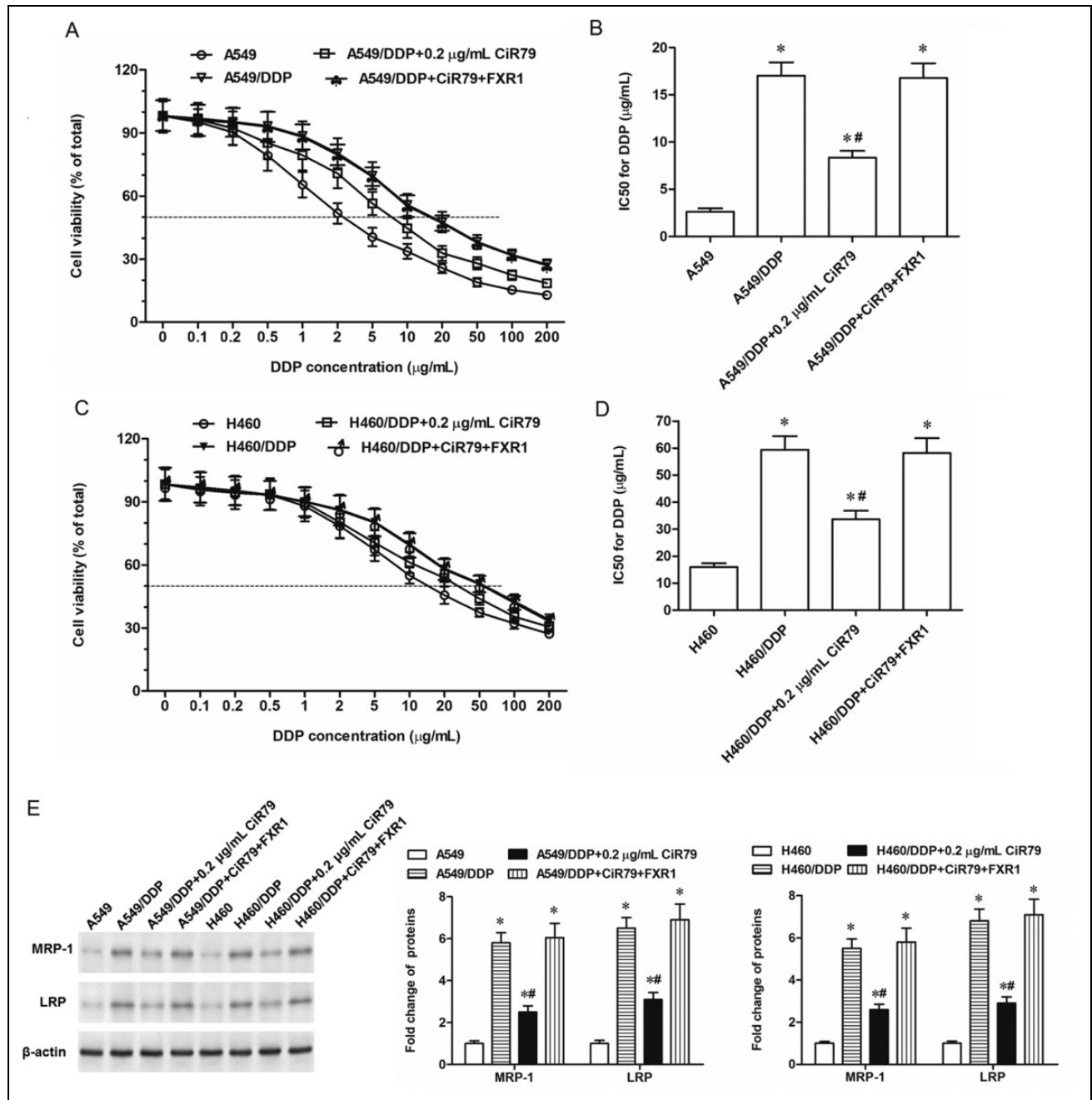


**Fig. 5.** FXR1 could restore the DDP resistance which was reduced by circ\_0000079. (A) A549, A549/DDP, and A549/DDP transfected with 0.2  $\mu\text{g/mL}$  pCDH-ciR79 and A549/DDP transfected with 0.2  $\mu\text{g/mL}$  pCDH-ciR79 plus 5  $\mu\text{g/mL}$  FXR1 recombinant protein were treated with DDP at the indicated concentrations for 48 h, and then the cell viability was detected by CCK-8. (B) The IC<sub>50</sub> for DDP in four types of cells ( $\mu\text{g/mL}$ ) ( $n = 6$ ). (C) H460, H460/DDP, and H460/DDP transfected with 0.2  $\mu\text{g/mL}$  pCDH-ciR79 and H460/DDP transfected with 0.2  $\mu\text{g/mL}$  pCDH-ciR79 and 5  $\mu\text{g/mL}$  FXR1 recombination protein were treated with DDP at the indicated concentrations for 48 h, and then the cell viability was detected by CCK-8 ( $n = 6$ ). (D) The IC<sub>50</sub> for DDP in four types of cells ( $\mu\text{g/mL}$ ) ( $n = 6$ ). (E) The levels of multidrug resistance-associated proteins MRP-1 and LRP were detected with Western blotting. \* $P < 0.05$  compared with nonresistant cell lines and # $P < 0.05$  compared with DDP-resistant cell strains. CCK-8: cell counting kit-8; DDP: cisplatin; FXR1: fragile X-related 1; IC<sub>50</sub>: half-maximal inhibitory concentration; LRP: lung resistance-associated protein; MRP-1: multidrug resistance-associated protein 1.

2013. However, whether circ\_0000079 is related to tumorigenesis remains to be further studied.

In this study, we observed significantly lower levels of circ\_0000079 in the tissues of NSCLC patients and

especially in drug-resistant NSCLC patients, and transfection with a circ\_0000079 overexpression vector inhibited cell proliferation and invasion in DDP-resistant NSCLC growth. The circ\_0000079 primer and probe were used to

RNA-IP and RNA pull-down showed that circ\_0000079 could bind with FXR1 but could not with PRCKI in NSCLC cells. Co-IP verified that FXR1 levels were increased but PRCKI levels had no change in the siCirc\_0000079 transfected cells, and Western blot assay revealed that circ\_0000079 regulated invasion and viability of NSCLC cells via interaction with FXR1. Our further studies suggested that resistance of NSCLC cells could be inhibited by circ\_0000079 overexpression, which could be restored by FXR1.

Recently, more papers indicated that circRNAs' unique covalently closed-loop structures and specific tertiary structures could act as a scaffold of modulating for binding with RNA-binding proteins, microRNAs, or other molecules, and thus they are involved in various aspects of cell physiology<sup>19,20</sup>. For instance, Schneider et al. discovered that several circRNAs were associated with the RNA-binding protein, insulin-like growth factor 2 binding protein 3, a known tumor marker<sup>21,22</sup>; Conn et al. identified the RNA-binding protein Quaking (QKI) as a major regulator of circRNA biogenesis in EMT, which is a cellular differentiation process important in embryo development, wound healing, and in cancer metastasis<sup>23</sup>. William et al. found that overexpression of circ-Foxo3 decreased the interaction between Foxo3 and MDM2 and repressed the function of MDM2 in modulating poly-ubiquitination of Foxo3<sup>23,24</sup>. In view of previous research ideas, we found that the uncharacterized circRNA circ\_0000079 could interact with the RNA-binding protein FXR1 in NSCLC cells.

RNA-binding proteins have profound implications for cellular physiology and multiple biological processes, and large-scale studies revealed that RNA-binding proteins play a role in post-transcriptional regulation and as a potential driver of tumor development<sup>23</sup>. As an example, Feng et al. discovered that QKI-5 regulates the alternative splicing of NUMB via binding to two RNA elements in its pre-mRNA, which in turn suppresses cell proliferation and prevents the activation of the Notch signaling pathway in lung cancer<sup>25,26</sup>. In addition, studies have found that the RNA-binding protein FXR1 was inversely correlated with patients' prognosis, and it was also highly expressed in many human cancers suggesting a role across multiple tumor types, including breast cancers, ovarian cancers, colon cancers, and so on<sup>14,15</sup>. A recent observation indicated that FXR1 was involved in the extracellular signal-related kinase (ERK) signaling pathway by directly interacting with PRCKI to promote cell proliferation, survival, and invasion of NSCLC cells<sup>14,27</sup>. Our current study demonstrated that circ\_0000079 could decoy FXR1 to inhibit the generation of FXR1/PRCKI complex in drug resistance NSCLC.

DDP is a member of platinum-containing anticancer drugs, and these platinum complexes react *in vivo* and cause DNA cross-linking, which ultimately triggers cell apoptosis<sup>28</sup>. DDP treatment demonstrates favorable outcomes initially, but later cancer cells rapidly obtain DDP resistance leading to relapse and therapeutic failure<sup>4,29</sup>. Drug

resistance could be caused by various mechanisms, such as a reduction in intracellular drug concentration, the activation of detoxifying systems, the activation of DNA repair, and the inhibition of apoptosis<sup>30,31</sup>. Recently, more studies have revealed that ERK signaling cascades play a critical role in the transmission of signals from growth factor receptors to prevent apoptosis, and it also proved that ERK signaling cascades may be a critical pathway conferring acquired drug resistance<sup>32-34</sup>. Furthermore, the FXR1/PRCKI complex could phosphorylate epithelial cell transforming 2 (ECT2) to activate ERK signaling cascades to drive transformed lung cancer cell growth and invasion<sup>14</sup>. Therefore, it is most likely that circ\_0000079 prevents the FXR1/PRCKI complex from activating the inhibitory apoptosis capacity of the ERK signaling in drug resistance NSCLC cells. Nevertheless, the suppressed drug resistance was restored by upregulated FXR1. In addition, FXR1 also participates in miRNA biogenesis, for example, FXR1 protein is required for the maturation of miR-9, miR-124, and miR-135. Thus, it could be the other regulatory mechanism that circ\_0000079 inhibited cell invasion and resistance in NSCLC. These speculations still need to be confirmed by further experiments.

The present paper showed, for the first time, that circ\_0000079 expression was downregulated and was associated with poor overall survival in NSCLC patients. Our findings further revealed that circ\_0000079 could decline the cell invasion and drug resistance in NSCLC by interrupting the formation of the FXR1/PRCKI complex by decoying FXR1. In conclusion, our studies suggested that circ\_0000079 holds great promise as a diagnostic and chemosensitivity target for drug-resistant NSCLC patients.

### Ethical Approval

This study was approved by the Ethics Committee at the Second Affiliated Hospital of Zhengzhou University (Zhengzhou, China).

### Statement of Human and Animal Rights

All procedures in this study were conducted in accordance with the Second Affiliated Hospital of Zhengzhou University of Institutional Review Board's (approval number: 00069) approved protocols.

### Statement of Informed Consent

Written informed consent was obtained from the patients for their anonymized information to be published in this article.


### Declaration of Conflicting Interests

The author(s) declared no potential conflicts of interest with respect to the research, authorship, and/or publication of this article.

### Funding

The author(s) received no financial support for the research, authorship, and/or publication of this article.

### ORCID iD

Chen Chen  <https://orcid.org/0000-0001-5943-9091>

## References

- Nie W, Ge HJ, Yang XQ, Sun X, Huang H, Tao X, Chen WS, Li B. LncRNA-UCA1 exerts oncogenic functions in non-small cell lung cancer by targeting miR-193a-3p. *Cancer Lett.* 2016; 371(1):99–106.
- Sullivan I, Planchard D. ALK inhibitors in non-small cell lung cancer: the latest evidence and developments. *Ther Adv Med Oncol.* 2016;8(1):32–47.
- Zhang S, Zeng X, Ding T, Guo L, Li Y, Ou S, Yuan H. Microarray profile of circular RNAs identifies hsa\_circ\_0014130 as a new circular RNA biomarker in non-small cell lung cancer. *Sci Rep.* 2018;8(1):2878.
- Liu D, Yan L, Wang L, Tai W, Wang W, Yang C. Genistein enhances the effect of cisplatin on the inhibition of non-small cell lung cancer A549 cell growth *in vitro* and *in vivo*. *Oncol Lett.* 2014;8(6):2806–2810.
- Reck M, Heigener DF, Mok T, Soria J-C, Rabe KF. Management of non-small-cell lung cancer: recent developments. *Lancet.* 2013;382(9893):709–719.
- Li W, Wang W, Ding M, Zheng X, Ma S, Wang X. MiR-1244 sensitizes the resistance of non-small cell lung cancer A549 cell to cisplatin. *Cancer Cell Int.* 2016;16(1):30.
- RybakWolf A, Stottmeister C, Glazar P, Jens M, Pino N, Giusti S, Hanan M, Behm M, Bartok O, Ashwal-Fluss R, Herzog M, et al. Circular RNAs in the mammalian brain are highly abundant, conserved, and dynamically expressed. *Mol Cell.* 2015; 58(5):870–875.
- Zhao F, Han Y, Liu Z, Zhao Z, Li Z, Jia K. circFADS2 regulates lung cancer cells proliferation and invasion via acting as a sponge of miR-498. *Biosci Rep.* 2018;38(4):BSR20180570.
- Qu S, Yang X, Li X, Wang J, Gao Y, Shang R, Sun W, Dou K, Li H. Circular RNA: a new star of noncoding RNAs. *Cancer Lett.* 2015;365(2):141–148.
- Ebbesen KK, Kjems J, Hansen TB. Circular RNAs: identification, biogenesis and function. *Biochim Biophys Acta.* 2016; 1859(1):163–168.
- Li J, Yang J, Zhou P, Le Y, Zhou C, Wang S, Xu D, Lin HK, Gong Z. Circular RNAs in cancer: novel insights into origins, properties, functions and implications. *Am J Cancer Res.* 2015; 5(2):472–480.
- Zong L, Sun Q, Zhang H, Chen Z, Deng Y, Li D, Zhang L. Increased expression of circRNA\_102231 in lung cancer and its clinical significance. *Biomed Pharmacother.* 2018;102: 639–644.
- Zhu X, Wang X, Wei S, Chen Y, Chen Y, Fan X, Han S, Wu G. hsa\_circ\_0013958: a circular RNA and potential novel biomarker for lung adenocarcinoma. *FEBS J.* 2017;284(14): 2170–2182.
- Qian J, Hassanein M, Hoeksema MD, Harris BK, Zou Y, Chen H, Lu P, Eisenberg R, Wang J, Espinosa A, Ji X, et al. The RNA binding protein FXR1 is a new driver in the 3q26-29 amplicon and predicts poor prognosis in human cancers. *Proc Natl Acad Sci U S A.* 2015;112(11):3469–3474.
- Comtesse N, Keller A, Diesinger I, Bauer C, Kayser K, Huwer H, Lenhof HP, Meese E. Frequent overexpression of the genes FXR1, CLAPM1 and EIF4G located on amplicon 3q26-27 in squamous cell carcinoma of the lung. *Int J Cancer.* 2007; 120(12):2538–2544.
- Jin X, Zhai B, Fang T, Guo X, Xu L. FXR1 is elevated in colorectal cancer and acts as an oncogene. *Tumour Biol.* 2016;37(2):2683–2690.
- You X, Conrad TO. Acfs: accurate circRNA identification and quantification from RNA-Seq data. *Sci Rep.* 2016;6(1):38820.
- Wang J, Li H. CircRNA circ\_0067934 silencing inhibits the proliferation, migration and invasion of NSCLC cells and correlates with unfavorable prognosis in NSCLC. *Eur Rev Med Pharmacol Sci.* 2018;22(10):3053–3060.
- Zhang HD, Jiang LH, Sun DW, Hou JC, Ji ZL. CircRNA: a novel type of biomarker for cancer. *Breast Cancer.* 2018;25(1): 1–7.
- Jeck WR, Sharpless NE. Detecting and characterizing circular RNAs. *Nat Biotechnol.* 2014;32(5):453–461.
- Tim S, Lee-Hsueh H, Silke S, Stefan S, Heinrich E, Oliver R, Stefan R, Jan M, Albrecht B. CircRNA-protein complexes: IMP3 protein component defines subfamily of circRNPs. *Sci Rep.* 2016;6:31313.
- Chen I, Chen CY, Chuang TJ. Biogenesis, identification, and function of exonic circular RNAs. *Wiley Interdiscip Rev RNA.* 2015;6(5):563–579.
- Conn SJ, Pillman KA, Toubia J, Conn VM, Salmanidis M, Phillips CA, Roslan S, Schreiber AW, Gregory PA, Goodall GJ. The RNA binding protein quaking regulates formation of circRNAs. *Cell.* 2015;160(6):1125–1134.
- Nieto MA. Epithelial plasticity: a common theme in embryonic and cancer cells. *Science.* 2013;342(6159):1234850.
- Narva E, Rahkonen N, Emani MR, Lund R, Pursiheimo JP, Nasti J, Autio R, Rasool O, Denessiouk K, Lahdesmaki H, Rao A, et al. RNA-binding protein L1TD1 interacts with LIN28 via RNA and is required for human embryonic stem cell self-renewal and cancer cell proliferation. *Stem Cells.* 2012; 30(3):452–460.
- Zong FY, Fu X, Wei WJ, Luo YG, Heiner M, Cao LJ, Fang Z, Fang R, Lu D, Ji H, Hui J. The RNA-binding protein QKI suppresses cancer-associated aberrant splicing. *PLoS Genet.* 2014;10(4):e1004289.
- Fields AP, Regala RP. Protein kinase C iota: human oncogene, prognostic marker and therapeutic target. *Pharmacol Res.* 2007;55(6):487–497.
- Apps MG, Choi EH, Wheate NJ. The state-of-play and future of platinum drugs. *Endocr Relat Cancer.* 2015;22(4): R219–R233.
- Galluzzi L, Senovilla L, Vitale I, Michels J, Martins I, Kepp O, Castedo M, Kroemer G. Molecular mechanisms of cisplatin resistance. *Oncogene.* 2012;31(15):1869–1883.
- Dong Z, Ren L, Lin L, Li J, Huang Y, Li J. Effect of microRNA-21 on multidrug resistance reversal in A549/DDP human lung cancer cells. *Mol Med Rep.* 2015;11(1):682–690.
- Xu Z, Mei J, Tan Y. Baicalin attenuates DDP (cisplatin) resistance in lung cancer by downregulating MARK2 and p-Akt. *Int J Oncol.* 2017;50(1):93–100.

32. Samatar AA, Poulikakos PI. Targeting RAS-ERK signalling in cancer: promises and challenges. *Nat Rev Drug Discov.* 2014; 13(12):928–942.
33. Montagut C, Settleman J. Targeting the RAF–MEK–ERK pathway in cancer therapy. *Cancer Lett.* 2009;283(2):125–134.
34. Mccubrey JA, Steelman LS, Abrams SL, Lee JT, Chang F, Bertrand FE, Navolanic PM, Terrian DM, Franklin RA, D’Assoro AB, Salisbury JL, et al. Roles of the RAF/MEK/ERK and PI3K/PTEN/AKT pathways in malignant transformation and drug resistance. *Adv Enzyme Regul.* 2006;46:249–279.
35. Xu XL, Zong R, Li Z, Biswas MHU, Fang Z, Nelson DL, Gao FB. FXR1P but not FMRP regulates the levels of mammalian brain-specific microRNA-9 and microRNA-124. *J Neurosci.* 2011;31(39):13705–13709.